Synthesis and Crystal Structure of Bis(1,1,1-tris(dimethylphosphinomethyl)ethane)iron(II) Tetrafluoroborate Dihydrate

Kazuo Kashiwabara,* Yuji Ozeki, Masakazu Kita,† Junnosuke Fujita,†† and Kiyohiko Nakajima†††

Department of Chemistry, Faculty of Science, Nagoya University, Chikusa-ku, Nagoya 464-01

†Naruto University of Education, Takashima, Naruto 772

††Division of Natural Sciences, International Christian University, Mitaka 181

†††Department of Chemistry, Aichi University of Education, Kariya 448

(Received July 27, 1995)

An air and thermally stable iron(II) complex of 1,1,1-tris(dimethylphosphinomethyl)ethane (mmtp), $[Fe(mmtp)_2](BF_4)_2\cdot 2H_2O$, has been prepared, and the crystal structure has been determined by X-ray analysis. The complex was crystallized in the orthorhombic, space group $Pca2_1$ with four molecules in a unit cell of dimensions $a=17.448(4)$, $b=17.574(4)$, $c=11.367(2)$ Å, and $V=3485(1)$ Å^3. Final R was 0.047 for 1671 reflections. The average Fe–P bond length of 2.312(5) Å is intermediate between those of $[Co(mmtp)_2][Co(CN)_6]\cdot 2.25H_2O$ (av Co–P=2.331(9) Å) and $[Cr(mmtp)_2]$ (av Cr–P=2.287(1) Å), in which Fe(II), Co(III), and Cr(0) have the same low-spin d^6 electron configuration. A less stable dimeric complex, $[Fe_2(\mu\text{-}Cl)_3(mmtp)_2]B(C_6H_5)_4\cdot H_2O$, has also been isolated. Absorption spectra and cyclic voltammograms have been compared between the Fe(II) and Co(III) complexes.

In previous studies,[1,2] we prepared a number of $[CoX_3(mmtp)]^{n+}$-type complexes, and determined the crystal structures of the complexes with X_3=mmtp, $(Cl)_3$, and $(CN)_3$. The structural study revealed that the Co–P bond lengths (av 2.331(9) Å) in $[Co(mmtp)_2]^{3+}$ were appreciably longer than the Cr–P ones (av 2.287(1) Å) in $[Cr(mmtp)_2]$,[3] both the Co(III) and Cr(0) having a low-spin d^6 electron configuration. The difference in the bond lengths was attributed to a difference in extent of the π-back donation from the metal to phosphorus donor atoms. In order to extend the study we have prepared $[Fe(mmtp)_2]^{2+}$, in which the Fe(II) ion also has a low-spin d^6 electron configuration, and determined the crystal structure in order to compare M–P bond lengths among these metal complexes. To our knowledge,[4] $[Fe(mmtp)_2]^{2+}$ is the first example of a mononuclear $[Fe(P)_6]^{2+}$-type complex, although several iron(II) complexes of a dimeric $[(P)_3Fe(\mu\text{-}X)_3Fe(P)_3]^{n+}$-type with similar tripod-type phosphine ligands ($(P)_3$), such as $[\{(MeC(CH_2PPh_2)_3)Fe\}_2(\mu\text{-}H)_3]BPh_4\cdot 2C_4H_8O$[5] and $[\{(MeC(CH_2PEt_2)_3)Fe\}_2(\mu\text{-}Cl)_3]BPh_4\cdot CH_2Cl_2$,[6] have been reported.

Experimental

The mmtp ligand was prepared by a literature method,[7] and handled under a N_2 atmosphere by the use of Schlenk techniques until its iron(II) complexes had formed. All of the solvents used for preparing the ligand and its complexes were made oxygen-free by bubbling nitrogen for 20 min immediately before use. The absorption as well as ^1H, ^{13}C, and ^{31}P NMR spectra were recorded on a Hitachi U3400 spectrophotometer and a R-90H spectrometer, respectively. Cyclic voltammograms were measured on a Fuso HECS 321B potential-sweep unit and a Fuso HECS 317B potentiostat at a scan rate 200 mV s^{-1} in CH_3CN solutions ([complex]: 1.0×10^{-3} mol dm^{-3}, 0.1 mol dm^{-3} Bu_4NBF_4) as those described in a previous paper.[8] A grassy-carbon disk, a platinum wire, and a Ag/Ag^+ electrode (Ag/0.01 mol dm^{-3} $AgNO_3$) were used as the working, auxiliary, and reference electrodes, respectively, the oxidation wave of ferrocene being observed at +0.09 V vs. Ag/Ag^+.

Preparation of the Complexes. $[Fe(mmtp)_2](BF_4)_2\cdot 2H_2O$. The mmtp ligand (1.0 g, 4.0 mmol) was added dropwise to a methanol solution (30 cm^3) of $FeCl_2$ (0.25 g, 2.0 mmol). The solution was refluxed for 5 h, and then diluted ten times with water. The unreacted free mmtp ligand was extracted with diethyl ether several times. The aqueous solution was applied to a column (ϕ3 cm×60 cm) of SP-Sephadex C-25 ion-exchange resin (Na^+ form), and the adsorbed products were eluted with an aqueous 0.2 mol dm^{-3} solution of $NaBF_4$. The eluate of the major yellow-orange band was evaporated to dryness under reduced pressure. From the residue a yellow-orange complex was extracted with nitromethane, and the extract

was evaporated again to dryness under reduced pressure. The product was recrystallized from acetone to give yellow-orange plate crystals. Yield 0.65 g (44%). Anal. Found: C, 34.46; H, 7.59%. Calcd for $C_{22}H_{58}B_2O_2F_8P_6Fe$: C, 34.32; H, 7.59%. ^{1}H NMR (CD_3CN) δ=1.20 (br. s, $-CH_3$), 1.61 (br. s, $P(CH_3)_2$), 1.74 (br. s, $-CH_2-$). $^{13}C\{^1H\}$ NMR (CD_3NO_2) δ=23.2 (br. s), 33.4 (s), 34.8 (qn.), 40.4 (t). ^{31}P NMR (CD_3CN) δ=7.33 ppm vs. 85% H_3PO_4. The complex is soluble in methanol, ethanol, acetonitrile, nitromethane, acetone, and water, but insoluble in dichloromethane and chloroform.

$[Fe_2(\mu\text{-}Cl)_3(mmtp)_2]B(C_6H_5)_4\cdot H_2O$. To a 1-butanol solution (30 cm^3) of $FeCl_2$ (0.25 g, 2.0 mmol) was added dropwise a dichloromethane solution (30 cm^3) of mmtp (0.50g, 2.0 mmol). The solution was stirred for 30 min, and then mixed with sodium tetraphenylborate (0.34 g, 1.0 mmol), yielding a red-violet precipitate. The precipitate was collected by filtration, and recrystallized from dichloromethane. Yield, 0.91 g (44%). Anal. Found: C, 52.07; H, 7.15%. Calcd for $C_{46}H_{76}BOP_6Cl_3Fe_2$: C, 52.13; H, 7.23%. The complex is soluble in dichloromethane, chloroform and acetone, but insoluble in water, methanol, and ethanol.

X-Ray Analysis. A crystal of $[Fe(mmtp)_2](BF_4)_2\cdot 2H_2O$ with approximate dimensions, 0.55×0.35×0.05 mm^3, grown from an acetone solution of the complex, was used for the data collection. The crystal data are: orthorhombic, $Pca2_1$, a=17.448(4), b=17.574(4), c=11.367(2) Å, V=3485(1) Å^3, D_x=1.47 g cm^{-3}, D_m=1.45 g cm^{-3}, Z=4, and μ(Mo $K\alpha$)=7.66 cm^{-1}. Diffraction data were collected on a Rigaku AFC-5R diffractometer with graphite monochromatized Mo $K\alpha$ radiation (λ=0.71073 Å). The θ–2θ scan technique was employed. A total of 2250 reflections within the range $2\theta<60°$ were measured, of which 1671 reflections were unique with $|F_o|>3\sigma(|F_o|)$. The positions of Fe and six P atoms were determined by direct methods (SHELXS-86[9]) and the remaining non-hydrogen atoms were located by the subsequent Fourier synthesis. The structure was refined by full-matrix least-squares techniques with anisotropic thermal parameters for the non-hydrogen atoms. All of the hydrogen atoms were located at the calculated positions with isotropic displacement parameters of their parent carbon atoms. The calculations were carried out with Xtal3.2[10] software. The refinement of the positional and thermal parameters converged to R=0.047 and R_w=0.056. The atomic parameters of non-hydrogen atoms are listed in Table 1. Tables of the anisotropic thermal parameters of non-hydrogen atoms and the observed and calculated structure factors are kept as Document No. 68069 at the Office of the Editor of Bull. Chem. Soc. Jpn.

Table 1. Positional Parameters and Equivalent Isotropic Displacement Parameters (Å^2) of $[Fe(mmtp)_2](BF_4)_2\cdot 2H_2O$

Atom	x/a	y/b	z/c	U_{eq}[a]
Fe	0.50803(9)	0.2542(1)	1/2	0.0205(5)
P(1)	0.4978(2)	0.3758(2)	0.5769(4)	0.028(1)
P(2)	0.4658(2)	0.2145(2)	0.6865(5)	0.028(1)
P(3)	0.6282(2)	0.2569(2)	0.5894(4)	0.029(1)
P(4)	0.3856(2)	0.2310(2)	0.4337(5)	0.028(1)
P(5)	0.5310(2)	0.3049(2)	0.3191(5)	0.029(1)
P(6)	0.5394(2)	0.1404(2)	0.4133(4)	0.030(1)
F(1)	0.3164(6)	0.4902(7)	0.314(1)	0.102(5)
F(2)	0.1889(6)	0.4632(7)	0.311(1)	0.096(5)
F(3)	0.2700(6)	0.3998(5)	0.195(1)	0.075(4)
F(4)	0.2435(6)	0.5252(5)	0.162(1)	0.072(4)
F(5)	0.3341(6)	−0.1501(6)	0.484(2)	0.117(6)
F(6)	0.3838(9)	−0.0511(7)	0.388(1)	0.125(7)
F(7)	0.3762(9)	−0.0477(8)	0.578(1)	0.128(7)
F(8)	0.2755(6)	−0.0411(6)	0.484(2)	0.132(7)
O(1)	0.250(1)	0.0453(7)	0.732(2)	0.136(8)
O(2)	0.3712(6)	0.3685(6)	1.000(1)	0.071(5)
C(1)	0.5696(9)	0.4443(7)	0.529(1)	0.036(5)
C(2)	0.4126(9)	0.4335(8)	0.562(2)	0.047(6)
C(3)	0.5114(9)	0.3837(9)	0.739(1)	0.037(6)
C(4)	0.5638(8)	0.3253(8)	0.800(1)	0.030(5)
C(5)	0.5223(9)	0.2495(8)	0.814(2)	0.031(5)
C(6)	0.458(1)	0.1130(9)	0.732(1)	0.044(6)
C(7)	0.3709(9)	0.2469(9)	0.736(1)	0.037(5)
C(8)	0.6363(9)	0.3158(8)	0.725(1)	0.033(6)
C(9)	0.6648(8)	0.1642(9)	0.647(1)	0.035(5)
C(10)	0.7151(7)	0.2895(8)	0.515(2)	0.044(6)
C(11)	0.5853(8)	0.3550(9)	0.919(1)	0.041(6)
C(12)	0.3054(8)	0.2958(8)	0.451(2)	0.045(6)
C(13)	0.3381(8)	0.1422(8)	0.484(2)	0.041(5)
C(14)	0.378(1)	0.2134(8)	0.274(2)	0.040(6)
C(15)	0.4479(8)	0.1792(7)	0.213(1)	0.029(5)
C(16)	0.5091(9)	0.2407(8)	0.192(2)	0.036(6)
C(17)	0.6241(9)	0.3403(9)	0.268(1)	0.042(6)
C(18)	0.472(1)	0.3879(9)	0.277(1)	0.045(6)
C(19)	0.4799(9)	0.1143(9)	0.285(1)	0.029(5)
C(20)	0.6337(9)	0.1350(9)	0.346(1)	0.045(6)
C(21)	0.5408(9)	0.0477(7)	0.491(2)	0.048(6)
C(22)	0.422(1)	0.1487(9)	0.089(2)	0.054(7)
B(1)	0.254(1)	0.471(1)	0.246(2)	0.047(7)
B(2)	0.345(1)	−0.076(1)	0.483(3)	0.055(8)

a) $U_{eq}=1/3\{\sum_i\sum_j U_{ij}\, a_i^* a_j^* \boldsymbol{a}_i\cdot\boldsymbol{a}_j\}$.

Results and Discussion

A yellow-orange and air and thermally stable iron(II) complex of the $[Fe(P)_6]^{2+}$-type, $[Fe(mmtp)_2]^{2+}$, was readily obtained by the reaction of mmtp with $FeCl_2$ in a molar ratio of 2 : 1 in methanol. The complex is stable in hot aqueous (60 °C) and 6 mol dm^{-3} HCl (20 °C) solutions. The ^{1}H, $^{13}C\{^1H\}$, and $^{31}P\{^1H\}$ NMR spectra show three, four and one kinds of signals for proton, carbon, and phosphorus nuclei, respectively, as described in Experimental. The spectral patterns of the ^{1}H and $^{13}C\{^1H\}$ NMR are similar to those for the corresponding Co(III) complex. Therefore, the Fe(II) complex can be assigned to a diamagnetic, low-spin d^6-type complex with six equivalent phosphorus donor atoms.

The reaction of mmtp with $FeCl_2$ in a molar ratio of 1 : 1 gave a red-violet complex. The complex which, was isolated as a $B(C_6H_5)_4^-$ salt, slowly changed to give yellow-orange $[Fe(mmtp)_2]^{2+}$ in solution at room temperature. An elemental analysis of the red-violet complex showed a composition of $[Fe_2(\mu\text{-}Cl)_3(mmtp)_2]B(C_6H_5)_4\cdot H_2O$, which is an analogue of the X-ray analyzed $[\{(MeC(CH_2PEt_2)_3)Fe\}_2(\mu\text{-}Cl)_3]BPh_4\cdot CH_2Cl_2$.[6] The absorption spectrum of the red-violet complex ex-

hibits the first ligand field band at 19000 cm^{-1} ($\log\varepsilon=3.03$), and the spectral pattern is similar to that of $[CoCl_3(mmtp)]$[1] in the 15000—30000 cm^{-1} region (1st band: 20100 cm^{-1} ($\log\varepsilon=3.18$)). Both the Fe(II) and Co(III) complexes of mmtp have the same low-spin d^6 electron configuration.

The crystal structure of yellow-orange $[Fe(mmtp)_2](BF_4)_2\cdot 2H_2O$ was determined by an X-ray analysis. Perspective views of the complex cation are shown in Fig. 1. The selected bond lengths and angles are given in Table 2. The Fe atom is surrounded by six phosphorus atoms of two facially coordinated tripod-type mmtp ligands to form a slightly distorted octahedron. The Fe(II)–P bond lengths are 2.277(5)—2.351(5) Å. The average value 2.312(5) Å is intermediate between those of the Co(III)–P bond lengths in $[Co(mmtp)_2][Co(CN)_6]\cdot 2.25H_2O$ (av Co–P=2.331(9) Å)[1] and the Cr(0)–P bond lengths in $[Cr(mmtp)_2]$ (av Cr–P=2.287(1) Å),[3] where all of the Fe(II), Co(III), and Cr(0) ions have a low-spin d^6 electron configuration. Since the M–P bonds in these complexes lengthen as the oxidation number of the central metal atom becomes higher, Cr(0)–P<Fe(II)–P<Co(III)–P, it is suggested that the contribution of π-back donation from the filled metal $d\pi$ orbitals (d^6) to the vacant phosphorus π orbitals (3d) is involved in these bonds. The metal $d\pi$ orbital energies in these complexes would increase in the order of Co(III)<Fe(II)<Cr(0), and the π-back donation would become more effective to strengthen the M–P bond in this order.

The structures of several Fe(II) complexes containing analogous tripod-type phosphine ligands have been determined by X-ray analysis. The Fe(II)–P bond lengths are 2.207(5)—2.235(5) Å (av 2.221(5) Å) for $[\{(MeC(CH_2PPh_2)_3)Fe\}_2(\mu\text{-}H)_3]PF_6\cdot 1.5CH_2Cl_2$,[5] 2.196(3)—2.211(3) Å (av 2.201(3) Å) for $[\{(MeC(CH_2PEt_2)_3)Fe\}_2(\mu\text{-}Cl)_3]BPh_4\cdot CH_2Cl_2$,[6] 2.181(6)—2.217(6) Å (av 2.201(6) Å) for $[\{MeC(CH_2PEt_2)_3\}Fe(\mu\text{-}\eta^3\text{-}P_3)Co\{MeC(CH_2PPh_2)_3\}](PF_6)_2\cdot CH_2Cl_2$,[11] and 2.154(2)—2.216(2) Å (av 2.177(2) Å) for $[\{(MeSi(CH_2PMe_2)_3)Fe\}_2(\mu\text{-}C{=}CH_2)(\mu\text{-}H)_2]$.[12] The Fe(II)–P bond lengths (av 2.312(5) Å) in $[Fe(mmtp)_2](BF_4)_2\cdot 2H_2O$ are much longer than those in these tripod phosphine complexes, and similar to those of the two mutually trans Fe(II)–P bonds (2.338(5) and 2.306(5) Å, av 2.322(5) Å) in $[FeCl_2\{P(CH_2CH_2CH_2PMe_2)_3\}]$.[13] The Fe(II)–P bonds trans to Cl^- in this complex are short, 2.202(5) and 2.231(5) Å (av 2.217(5) Å). Thus, the long Fe(II)–P bonds in $[Fe(mmtp)_2](BF_4)_2\cdot 2H_2O$ can be attributed to the strong trans influence of the phosphino group, although the crowded structure around the metal ion arising from the six dimethylphosphino donor groups may be an additional factor of lengthening the Fe(II)–P bonds.

The chelate conformations and angles of mmtp in $[Fe(mmtp)_2]^{2+}$ are quite similar to those in $[Co(mmtp)_2][Co(CN)_6]\cdot 2.25H_2O$.[1] As shown in Fig. 1(b), the two mmtp ligands are twisted to the same hand around the C_3 axis, affording chirality of the complex ion, although the crystals are a racemate which consists of a pair of enantiomers in the unit cell. The bite angles of mmtp are 83.4(2)—86.4(2)° (av 84.9(2)°). The cis P–Fe–P angles formed by two mmtp ligands are classified into two groups, 87.2(2), 89.5(2), 89.6(2)° (av 88.8(2)°) and 101.7(2), 102.5(2), 103.2(2)° (av 102.5(2)°). The three small and three large angles are arranged alternatively when viewed from the direction of the chemical C_3 axis. The torsion angles of the Fe–P–C–C moieties are 26(1)—30(1)° (av 28(1)°). These values are very similar to those found for $[Co(mmtp)_2]^{3+}$.[1]

The absorption spectrum of $[Fe(mmtp)_2](BF_4)_2$ is compared with that of $[Co(mmtp)_2]^{3+}$ in Fig. 2. Two

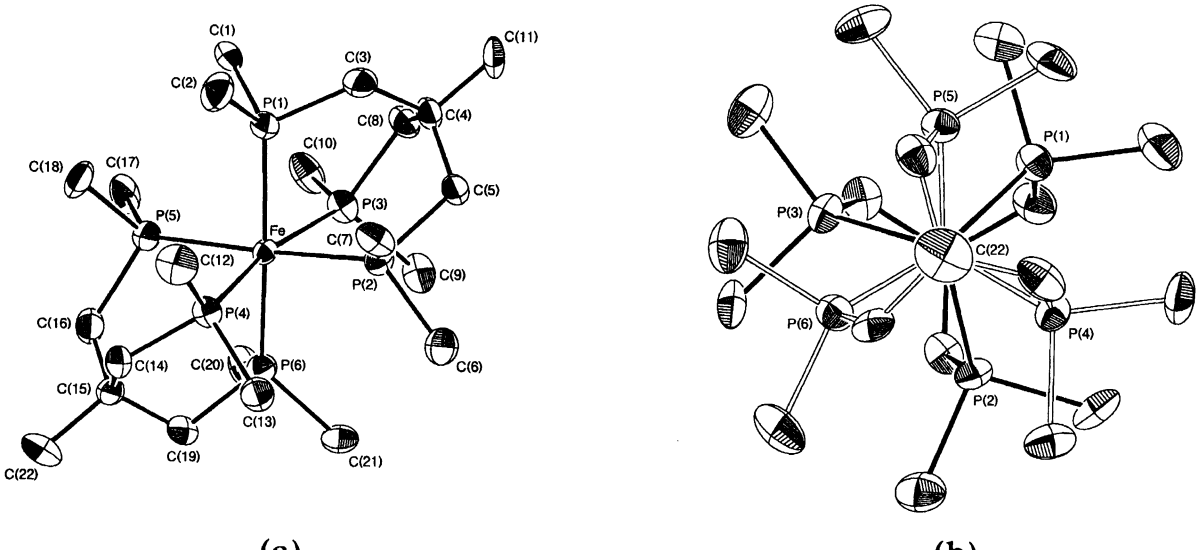

Fig. 1. Perspective views of the complex cation in $[Fe(mmtp)_2](BF_4)_2\cdot 2H_2O$.

Table 2. Selected Bond Distances (l/Å) and Bond Angles (ϕ/°) of $[Fe(mmtp)_2](BF_4)_2 \cdot 2H_2O$

	Distance		Distance
Fe–P(1)	2.316(4)	P(5)–C(18)	1.85(2)
Fe–P(2)	2.351(5)	P(6)–C(19)	1.85(2)
Fe–P(3)	2.331(4)	P(6)–C(20)	1.82(2)
Fe–P(4)	2.302(4)	P(6)–C(21)	1.85(1)
Fe–P(5)	2.277(5)	C(3)–C(4)	1.54(2)
Fe–P(6)	2.296(4)	C(4)–C(5)	1.52(2)
P(1)–C(1)	1.82(1)	C(4)–C(8)	1.53(2)
P(1)–C(2)	1.81(2)	C(4)–C(11)	1.49(2)
P(1)–C(3)	1.87(2)	C(14)–C(15)	1.53(2)
P(2)–C(5)	1.85(2)	C(15)–C(16)	1.54(2)
P(2)–C(6)	1.86(2)	C(15)–C(19)	1.51(2)
P(2)–C(7)	1.84(2)	C(15)–C(22)	1.57(2)
P(3)–C(8)	1.87(2)	F(1)–B(1)	1.37(3)
P(3)–C(9)	1.87(2)	F(2)–B(1)	1.37(3)
P(3)–C(10)	1.83(1)	F(3)–B(1)	1.40(2)
P(4)–C(12)	1.82(1)	F(4)–B(1)	1.36(2)
P(4)–C(13)	1.86(1)	F(5)–B(2)	1.31(2)
P(4)–C(14)	1.85(2)	F(6)–B(2)	1.35(3)
P(5)–C(16)	1.87(2)	F(7)–B(2)	1.32(3)
P(5)–C(17)	1.83(2)	F(8)–B(2)	1.36(2)
	Angle		**Angle**
P(1)–Fe–P(2)	84.8(1)	C(20)–P(6)–C(21)	98.1(7)
P(1)–Fe–P(3)	83.4(2)	P(1)–C(3)–C(4)	118(1)
P(1)–Fe–P(4)	102.5(2)	C(3)–C(4)–C(5)	110(1)
P(1)–Fe–P(5)	89.6(2)	C(3)–C(4)–C(8)	108(1)
P(1)–Fe–P(6)	169.8(2)	C(3)–C(4)–C(11)	109(1)
P(2)–Fe–P(3)	84.0(1)	C(5)–C(4)–C(8)	111(1)
P(2)–Fe–P(4)	87.2(2)	C(5)–C(4)–C(11)	110(1)
P(2)–Fe–P(5)	170.4(2)	C(8)–C(4)–C(11)	109(1)
P(2)–Fe–P(6)	101.7(2)	P(2)–C(5)–C(4)	118(1)
P(3)–Fe–P(4)	168.9(2)	P(3)–C(8)–C(4)	117(1)
P(3)–Fe–P(5)	103.2(2)	P(4)–C(14)–C(15)	117(1)
P(3)–Fe–P(6)	89.5(2)	C(14)–C(15)–C(16)	110(1)
P(4)–Fe–P(5)	86.4(2)	C(14)–C(15)–C(19)	110(1)
P(4)–Fe–P(6)	85.8(2)	C(14)–C(15)–C(22)	108(1)
P(5)–Fe–P(6)	84.9(2)	C(16)–C(15)–C(19)	111(1)
C(1)–P(1)–C(2)	99.6(7)	C(16)–C(15)–C(22)	108(1)
C(1)–P(1)–C(3)	99.2(7)	C(19)–C(15)–C(22)	110(1)
C(2)–P(1)–C(3)	98.8(8)	P(5)–C(16)–C(15)	116(1)
C(5)–P(2)–C(6)	97.9(7)	P(6)–C(19)–C(15)	117(1)
C(5)–P(2)–C(7)	98.0(7)	F(1)–B(1)–F(2)	112(2)
C(6)–P(2)–C(7)	98.5(7)	F(1)–B(1)–F(3)	108(2)
C(8)–P(3)–C(9)	99.7(7)	F(1)–B(1)–F(4)	109(2)
C(8)–P(3)–C(10)	98.4(7)	F(2)–B(1)–F(3)	107(1)
C(9)–P(3)–C(10)	98.7(6)	F(2)–B(1)–F(4)	109(2)
C(12)–P(4)–C(13)	98.7(6)	F(3)–B(1)–F(4)	111(2)
C(12)–P(4)–C(14)	98.9(8)	F(5)–B(2)–F(6)	114(2)
C(13)–P(4)–C(14)	97.4(7)	F(5)–B(2)–F(7)	115(2)
C(16)–P(5)–C(17)	98.0(7)	F(5)–B(2)–F(8)	109(2)
C(16)–P(5)–C(18)	99.4(7)	F(6)–B(2)–F(7)	109(2)
C(17)–P(5)–C(18)	98.3(8)	F(6)–B(2)–F(8)	108(2)
C(19)–P(6)–C(20)	99.6(7)	F(7)–B(2)–F(8)	101(2)
C(19)–P(6)–C(21)	99.5(7)		

absorption peaks at 23300 cm^{-1} ($\log \varepsilon$=2.73) and 28200 cm^{-1} ($\log \varepsilon$=2.35) for $[Fe(mmtp)_2]^{2+}$ can be assigned to the first and second d–d absorption bands, respectively, from comparisons with peak positions and intensities of

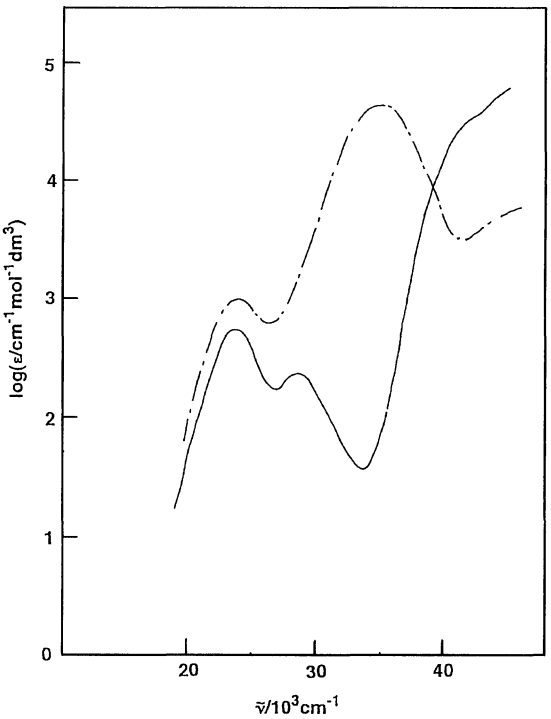

Fig. 2. Absorption spectra of $[Fe(mmtp)_2](BF_4)_2 \cdot 2H_2O$ in CH_3CN (—) and $[Co(mmtp)_2](BF_4)_3$ in H_2O (---).

low-spin d^6 Fe(II) complexes. The first absorption band is slightly lower in energy than that of $[Co(mmtp)_2]^{3+}$ (24000 cm^{-1}, $\log \varepsilon$=2.92), which is the same low-spin d^6 complex. The energy ratio of the first band of the Fe(II) to that of the Co(III) complex (23300 cm^{-1}/24000 cm^{-1}=0.971) almost agrees with the Shimura's spectrochemical parameter m for Fe(II), 0.965.[14] Strong absorptions in the high energy region (>ca. 40000 cm^{-1}) of $[Fe(mmtp)_2]^{2+}$ seem to correspond to the strong band around 35000 cm^{-1} of $[Co(mmtp)_2]^{3+}$ which can be assigned to charge transfer transitions from the ligand(σ) to Co(III)($d\sigma^*$) (LMCT). Since the 3d orbital energies of Fe(II) will be higher than those of Co(III), absorptions due to LMCT in $[Fe(mmtp)_2]^{2+}$ will be shifted to the higher energy side. For Fe(II) complexes, however, charge-transfer transitions from the metal (filled $d\pi$) to ligand (vacant σ^* or π^* orbital) (MLCT) may also be possible. It is not clear at present whether the strong absorptions of the Fe(II) complex are LMCT or MLCT.

Figure 3 compares cyclic voltammograms of $[Fe(mmtp)_2]^{2+}$ and $[Co(mmtp)_2]^{3+}$ in CH_3CN. One and two reversible one-electron waves were observed for $[Fe(mmtp)_2]^{2+}$ and $[Co(mmtp)_2]^{3+}$, respectively. The $E_{1/2}$ value of 0.87 V in (A) can be assigned to the Fe^{2+}/Fe^{3+} couple, and those of −0.57 V and −0.86 V in (B) to the Co^{3+}/Co^{2+} and Co^{2+}/Co^{+} couples, respectively. Other redox waves were not observed in the range of voltage limits (ca. −2.0—+1.8 V vs. Ag/Ag^+) of CH_3CN. The oxidation potential of $[Fe(mmtp)_2]^{2+}$ is related to the $d\pi$ orbital energy (HOMO), while the two reduction

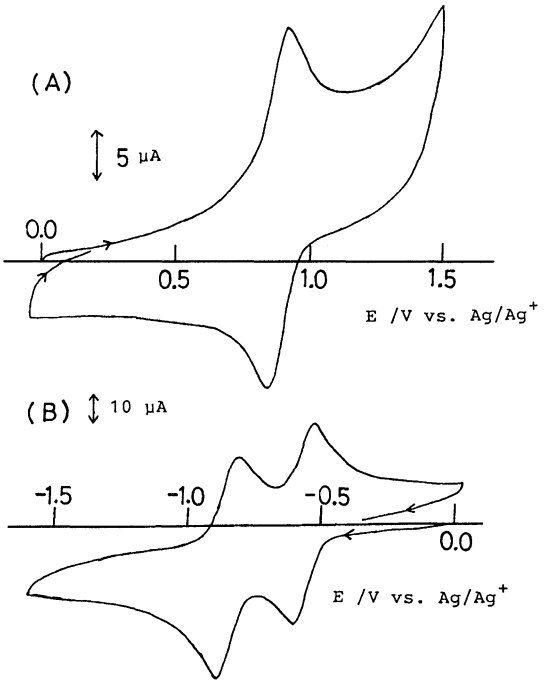

Fig. 3. Cyclic voltammograms of (A) $[Fe(mmtp)_2](BF_4)_2 \cdot 2H_2O$ and (B) $[Co(mmtp)_2](BF_4)_3$, in CH_3CN.

potentials of $[Co(mmtp)_2]^{3+}$ to the $d\sigma^*$ orbital energy (LUMO). As shown in the absorption spectra, the energy differences between the $d\pi$ and $d\sigma^*$ orbitals are similar in these two complexes. It can thus be concluded that the 3d orbitals ($d\pi$ and $d\sigma^*$) of the Co(III) complex are at appreciably lower energy than those of the Fe(II) complex.

We wish to thank Institute for Molecular Science (Okazaki) for the use of X-ray and computation facilities. The present work was partially supported by Grants-in-Aid for Scientific Research Nos. 06453048, 06640727, and 07554061 from the ministry of Education, Science and Culture.

References

1) T. Ando, M. Kita, K. Kashiwabara, J. Fujita, S. Kurachi, and S. Ohba, *Bull. Chem. Soc. Jpn.*, **65**, 2748 (1992).

2) K. Kashiwabara, M. Kita, J. Fujita, S. Kurachi, and S. Ohba, *Bull. Chem. Soc. Jpn.*, **67**, 2145 (1994).

3) A. M. Arif, J. G. Hefner, R. A. Jones, and B. R. Whittlesey, *Inorg. Chem.*, **25**, 1080 (1986).

4) P. N. Hawker and M. V. Twigg, "Comprehensive Coordination Chemistry," ed by G. Wilkinson, R. D. Gillard, and J. A. McCleverty, Pergamon Press, Oxford (1987), Vol. 4, Chap. 44.1.

5) P. Dapporto, S. Midollini, and L. Sacconi, *Inorg. Chem.*, **14**, 1643 (1975).

6) C. Bianchini, P. Dapporto, C. Mealli, and A. Meli, *Inorg. Chem.*, **21**, 612 (1982).

7) G. M. Whitesides, C. P. Casey, and J. K. Krieger, *J. Am. Chem. Soc.*, **93**, 1379 (1971).

8) M. Okuno, M. Kita, K. Kashiwabara, and J. Fujita, *Chem. Lett.*, **1989**, 1643.

9) G. M. Sheldrick, "A Program for the Solution of Crystal Structures from Diffraction Data," University of Göttingen, 1986.

10) S. R. Hall, H. D. Flack, and J. M. Stewart, "Xtal3.2, Program for X-Ray Crystal Structure Analysis," Universities of Western Australia, Geneva, and Maryland (1992).

11) C. Bianchini, M. Di Vaira, A. Meli, and L. Sacconi, *Inorg. Chem.*, **20**, 1169 (1981).

12) J. M. Boncella, M. L. H. Green, and D. O'Hare, *J. Chem. Soc., Chem. Commun.*, **1986**, 618.

13) M. Antberg and L. Dahlenburg, *Inorg. Chim. Acta*, **104**, 51 (1985).

14) Y. Shimura, *Bull. Chem. Soc. Jpn.*, **61**, 693 (1988).